

# RSC Advances



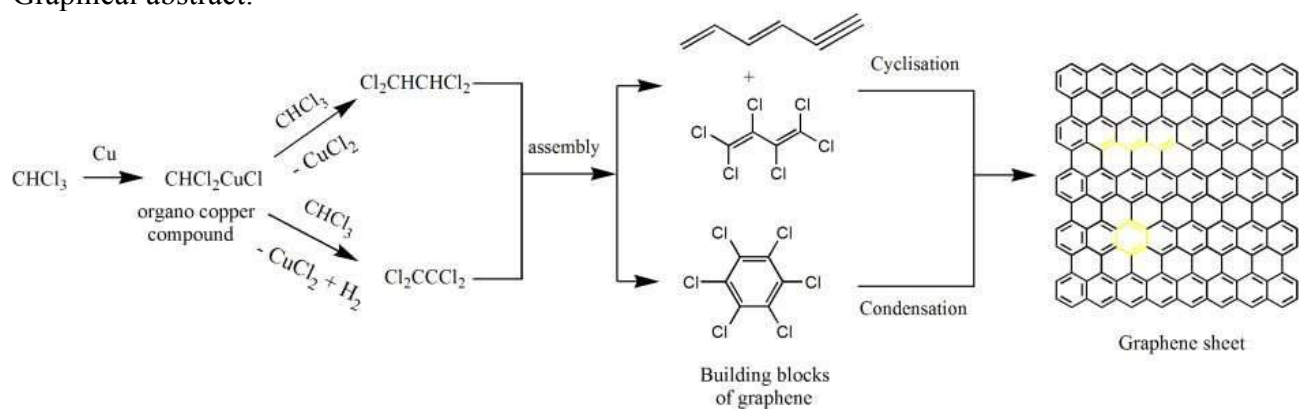
This is an *Accepted Manuscript*, which has been through the Royal Society of Chemistry peer review process and has been accepted for publication.

*Accepted Manuscripts* are published online shortly after acceptance, before technical editing, formatting and proof reading. Using this free service, authors can make their results available to the community, in citable form, before we publish the edited article. This *Accepted Manuscript* will be replaced by the edited, formatted and paginated article as soon as this is available.

You can find more information about *Accepted Manuscripts* in the [Information for Authors](#).

Please note that technical editing may introduce minor changes to the text and/or graphics, which may alter content. The journal's standard [Terms & Conditions](#) and the [Ethical guidelines](#) still apply. In no event shall the Royal Society of Chemistry be held responsible for any errors or omissions in this *Accepted Manuscript* or any consequences arising from the use of any information it contains.

Graphical abstract:



**Low temperature bottom-up approach for the synthesis of few layered graphene  
nanosheets via C–C bond formation using a modified Ullmann reaction**

Sandesh Y. Sawant <sup>a, b</sup>, Rajesh S. Somani <sup>a\*</sup>, Moo Hwan Cho <sup>b\*</sup> and Hari C. Bajaj <sup>a\*</sup>

<sup>a</sup> Division of Inorganic Materials and Catalysis,

Central Salt & Marine Chemicals Research Institute,

Council of Scientific & Industrial Research (CSIR),

G. B. Marg, Bhavnagar 364002, Gujarat, India.

<sup>b</sup> School of Chemical Engineering, Yeungnam University,

Gyeongsan-si, Gyeongbuk 712-749, South Korea

---

\* Corresponding author: Tel: +91 278 2471793; Fax: +91 278 2567562; E-mail:

[rssomani@csmcri.org](mailto:rssomani@csmcri.org) (Rajesh S. Somani); [hcbajaj@csmcri.org](mailto:hcbajaj@csmcri.org) (Hari C. Bajaj); Tel: +82-53-

810-2517; Fax: +82-53-810-4631; E-mail: [mhcho@ynu.ac.kr](mailto:mhcho@ynu.ac.kr) (Moo Hwan Cho)

The present address of Sandesh Y. Sawant is School of Chemical Engineering, Yeungnam

University, Gyeongsan-si, Gyeongbuk 712-749, South Korea

## Abstract

A low temperature, single-pot, bottom-up approach for the synthesis of few layered graphene sheets using the modified Ullmann reaction is reported. The synthesis protocol involved a solvothermal technique under an autogenic pressure of chloroform, which was used as the carbon source. Scanning and transmission electron microscopy revealed the formation of randomly aggregated, thin, crumpled graphene sheets with a thickness of ~2 nm. Solid state  $^{13}\text{C}$  nuclear magnetic resonance and Fourier transform infrared spectroscopy showed that the prepared graphene sheets have copious surface functionality. The possible growth mechanism for the formation of graphene sheets is proposed based on an analysis of the intermediate products by gas chromatography coupled with mass spectroscopy. The growth of few layered graphene sheets proceeded through the addition and cyclisation reactions of different chloroalkene intermediate products formed by the addition reaction of chloroform molecules, and not by the chain polymerization of chloroform molecules.

**Keywords:** Dechlorination; Nanosheets; Chloroform; Growth mechanism

## 1. Introduction

Graphene is the building block of many carbon-based nanomaterials, such as carbon nanotubes and fullerenes.<sup>1</sup> Graphene is the individual sheet of graphite with a hexagonal two-dimensional network of  $sp^2$ - hybridized carbon atoms with atomic thickness.<sup>2,3</sup> Graphene based materials offer new opportunities in the field of science and technology because of their excellent mechanical and electrical properties.<sup>4,5</sup> Graphene has been reported as a promising candidate for nanoelectronics and spintronics devices.<sup>6-9</sup> Graphene has also been used as a substitute for carbon nanotubes for reinforcement in polymer composites.<sup>10</sup>

Over the last few decades, many attempts have been made for the production of individual and functionalized graphene sheets.<sup>11</sup> The methods reported for the synthesis of graphene sheets include the chemical and mechanical exfoliation of graphite<sup>12</sup> and vacuum graphitization of silicon carbide.<sup>13, 14</sup> Recently, the chemical reduction of graphite oxide,<sup>15</sup> pyrolysis of camphor under reducing conditions<sup>16</sup> and inductively coupled radio-frequency plasma enhanced chemical vapor deposition<sup>17</sup> have been used for the fabrication of graphene. In most of these methods, the starting material was either graphite or graphite oxide prepared by an acid treatment of graphite, which resulted in graphene after further thermal or mechanical treatments.<sup>16, 18</sup> Many of the techniques used for the graphene synthesis involved multi-steps or required either high temperature or advanced and expensive instrument facilities.<sup>16, 17</sup> The solvothermal method is a cost-effective technique for the synthesis of different carbon nanostructures.<sup>19,20</sup> Choucair et al.<sup>21</sup> reported the first solvothermal approach for the gram-scale production of graphene, which involved the solvothermal preparation followed by a sonication

treatment. Recently, the synthesis of few layered graphene sheets using the solid state dechlorination of hexachloro ethane was reported.<sup>22</sup>

This paper describes the synthesis of few layered graphene sheets with a modified Ullmann reaction using chloroform as the carbon source, treated with metallic copper under a solvothermal condition. A possible mechanism to illustrate the graphene sheets formation based on the available literature and analysis results is proposed.

## 2. Experimental

### 2.1. Synthesis of few layered graphene sheets

All chemicals were procured from S. D. Fine Chem., India and used as received. In a typical experiment, metallic copper powder (10 g, 99.7% pure) and  $\text{CHCl}_3$  (25 mL) were heated to 200 °C for 10 h in a Teflon<sup>®</sup> lined stainless steel autoclave with a 55 ml capacity. After the reaction, the autoclave was cool to room temperature. The resulting reaction mass was filtered carefully and the mother liquor was collected for further analysis. The product was treated with a 6 M  $\text{HNO}_3$  solution at room temperature for 12 h, followed by filtration and washing the residues with distilled water several times to obtain a filtrate with a neutral pH and chloride free. Finally, the solid mass was air dried at 100 °C for 10 h. The final yield of the carbon product was approximately 0.9 g.

### 2.2. Characterization

The phase and crystallography of the products were characterized by X-ray diffraction (XRD, PHILIPS X'Pert MPD) using  $\text{CuK}\alpha_1$  radiation ( $\lambda = 1.54056 \text{ \AA}$ ), at a scanning rate of  $0.05^\circ\text{s}^{-1}$  in the  $2\theta$  range, 2–80°. The morphology of the samples was examined by scanning

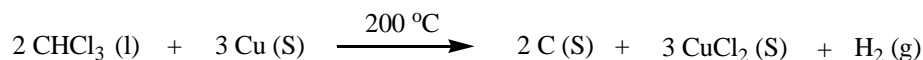
electron microscopy (SEM, Leo 1430 SEM). Transmission electron microscopy (TEM, JEOL JEM-2100 TEM) was performed at an accelerating voltage of 200 kV. For TEM analysis, a dilute suspension of the graphene sheets was prepared in acetone using an ultra-sonication technique and 0.2 ml of the solution was dropped on a wholly carbon coated copper grid and dried under ambient conditions.

The surface functionality of the graphene sheets was examined by the Fourier Transform infrared (FT-IR) spectroscopy (Perkins Elmer Spectrum GX 2500 FT-IR spectrophotometer). The  $^{13}\text{C}$  magic angle spinning – nuclear magnetic resonance (MAS-NMR) spectrum was recorded on a Bruker 500 MHz Advanced II spectrometer with a 5 mm MAS probe. The spectrum was acquired with cross polarization for a spinning speed of 8 KHz with 2 ms and 5s as the contact and recycle time, respectively. Line broadening of 200 Hz was applied and the spectrum was referenced to adamantane as a standard. The mother liquor of the reaction was analyzed by gas chromatography equipped with mass spectroscopy (GC-MS, GCMS-QP 2010, Shimadzu) using helium as the carrier gas for qualitative and quantitative analysis of the reaction intermediates. The textural properties were measured by the  $\text{N}_2$  adsorption-desorption method using a volumetric gas adsorption apparatus (ASAP 2020, Micromeritics Inc. USA). The pore size distribution was estimated using the Barrett–Joyner Halenda (BJH) model. Thermogravimetric analysis (TGA, Mettler Toledo TGA/SDTA 851) was performed under a nitrogen flow (50 ml/min) at a heating rate of 10 °C/min. The elemental composition of the few layered graphene sheets was determined by CHN/O/Cl analysis (Vario Micro Cube, Elementar, Germany) and the surface composition was obtained by Energy Dispersive X-ray (EDX) analysis assembled with SEM.

### 3. Results and discussion

#### 3.1. Synthesis of few layered graphene sheets

The classical Ullmann reaction involves the copper catalyzed synthesis of symmetrical biaryls at 200 °C.<sup>23</sup> This paper reports a new pathway for the synthesis of few layered graphene sheets using a modification of the classical Ullmann reaction. The synthesis was carried out under solvothermal conditions, in which chloroform reacts with copper under an autogenic vapor pressure. Few layered graphene sheets prepared using the modified Ullmann reaction under solvothermal conditions was proposed to crystallize according to the reaction pathway given below:



$\text{CHCl}_3$  was used as both the carbon source and solvent, and Cu was used as the reductant for the formation of graphene sheets.

#### 3.2. XRD analysis

The XRD pattern of the product prepared using chloroform (Fig.1a) show a broad peak in the  $2\theta$  range, 15–35°, instead of a comparatively sharp peak for typical graphitic planes at  $2\theta = 26.5^\circ$  (JCPDS 41-1487), revealing a few layer structure in addition to the amorphous nature of the graphene sheets.<sup>16</sup> The smooth peak shown in Fig. 1(a) is a Lorentzian fit for the obtained XRD pattern and centered at  $2\theta = 26^\circ$ . The broadness of this peak indicates the disorder structure and low degree of graphitization of the prepared graphene sheets. The low reaction temperature



is mainly responsible for the lower degree of graphitization of the prepared graphene sheets and was also observed for the different carbon nanostructures produced using low temperature dechlorination pathway.<sup>24-26</sup> Ju et al.<sup>27</sup> and Xi et al.<sup>28</sup> observed that the crystallinity or graphitization of the carbon products including nanosheets, nanobelts and nanocables was highly dependent on the reaction temperature and increases with increase in reaction temperature. The average thickness and number of layers of the prepared graphene sheets was calculated by fitting the peak obtained for (0 0 2) plane with the Scherrer formula. The approximate sheet thickness was  $\sim 2$  nm and the number of layers in the graphene sample was  $\sim 5$ -6.<sup>16</sup> The formation of copper chloride (JCPDS No. 79-1635 please check compare) during the reaction due to reductive elimination of chlorine from chloroform was confirmed by XRD analysis of the reaction mass obtained before the acid treatment (Fig. 1b). The similar results have been reported by Kuang et al.<sup>29</sup> for the formation of KCl salt as by-product during the synthesis of carbon nanosheets using carbon tetrachloride and metallic potassium under solvothermal condition.

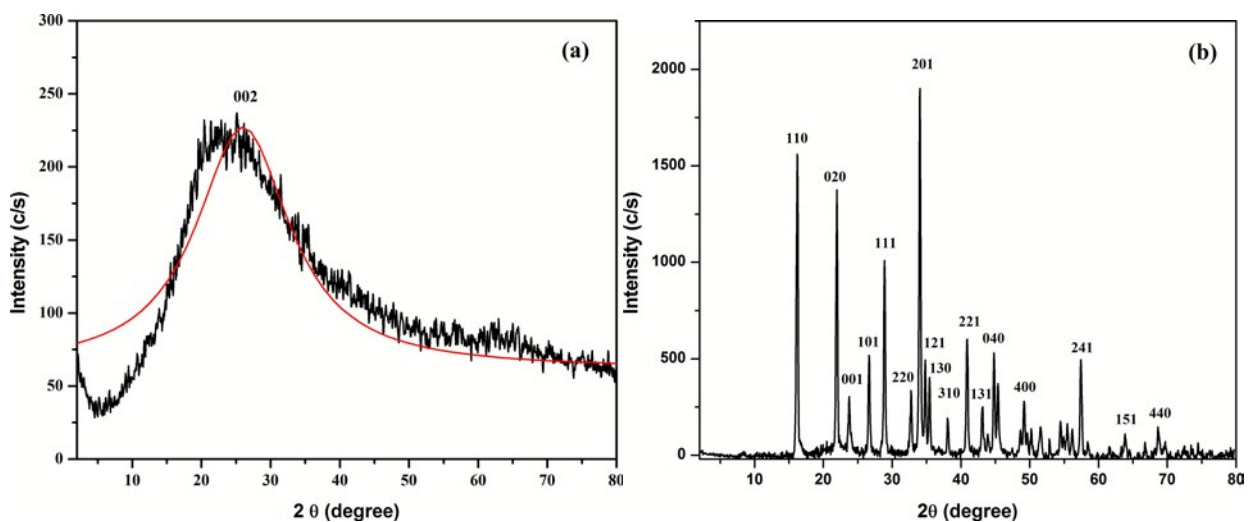


**Fig. 1** XRD pattern of (a) few layered graphene sheets prepared from chloroform in presence of copper using modified Ullmann reaction with a Lorentzian fit (smooth line) and (b) product without any post synthesis-acid treatment.

### 3.3. Microscopic analysis

SEM analysis of the product obtained from the present methodology (Fig. 2) revealed randomly aggregated, thin, crumpled sheets closely associated with each other forming a disordered particle. It is well-known that the synthesis of graphene sheets from dechlorination or solvothermal route generally yields three dimensional particles containing crumpled few layered graphene sheets rather than separated and single layer graphene sheets due to their disorder and multi-directional growth.<sup>29,30</sup> Fig. 2 clearly showed that the obtained graphene sheets have sharp edges and many folds. The obtained product showed the intercalated graphene sheets might be due to the absence of the flat support such as catalyst film,<sup>31</sup> Si or quartz<sup>32</sup> and metal substrate<sup>33</sup> during solvothermal reaction condition. Similar type of observation has also reported by Kuang et al.<sup>29</sup> for the synthesis of carbon nanosheets using carbon tetrachloride under solvothermal condition. Further analysis by TEM (Fig. 3) showed the presence of large, disordered, crinkled few layered graphene sheets. The average thickness of the graphene sheets (determined with folded region) was ~ 2 nm (Fig. 3b), which is in accordance with the XRD results. The ring type selected area electron diffraction pattern of the graphene sheets (inset in Fig. 3b) revealed the crumpling and disordered arrangement of the product.<sup>34</sup>

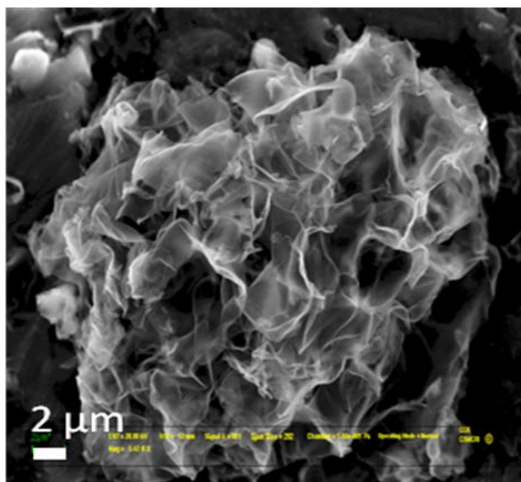


**Fig. 2** SEM image of agglomerated crumpled graphene sheets prepared at 200 °C under solvothermal condition.

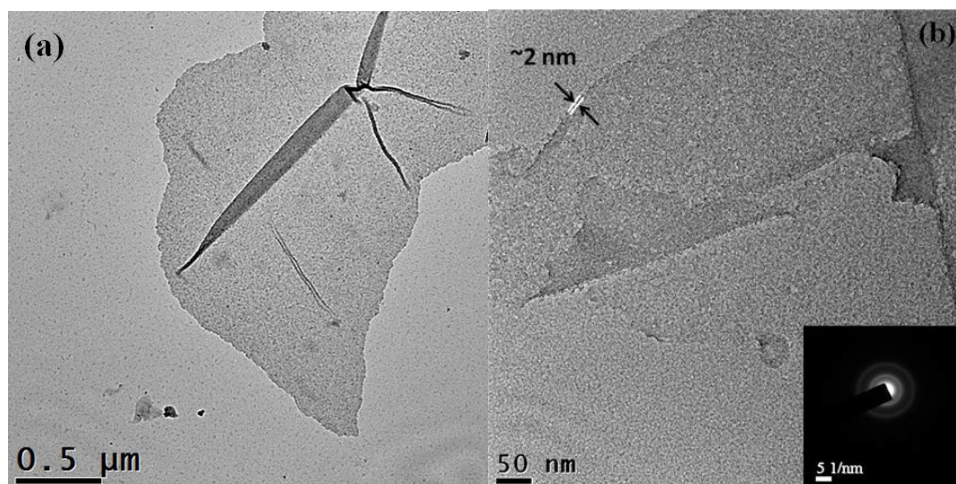


**Fig. 3** TEM images of (a) individual few layered graphene sheet with folds and few micrometers in length, and (b) curled graphene sheet with a crumpling edge of ~ 2 nm (The inset picture shows the ring type SAED pattern of the graphene sheets observed for Fig. 3b).

### 3.4. Spectroscopic analysis

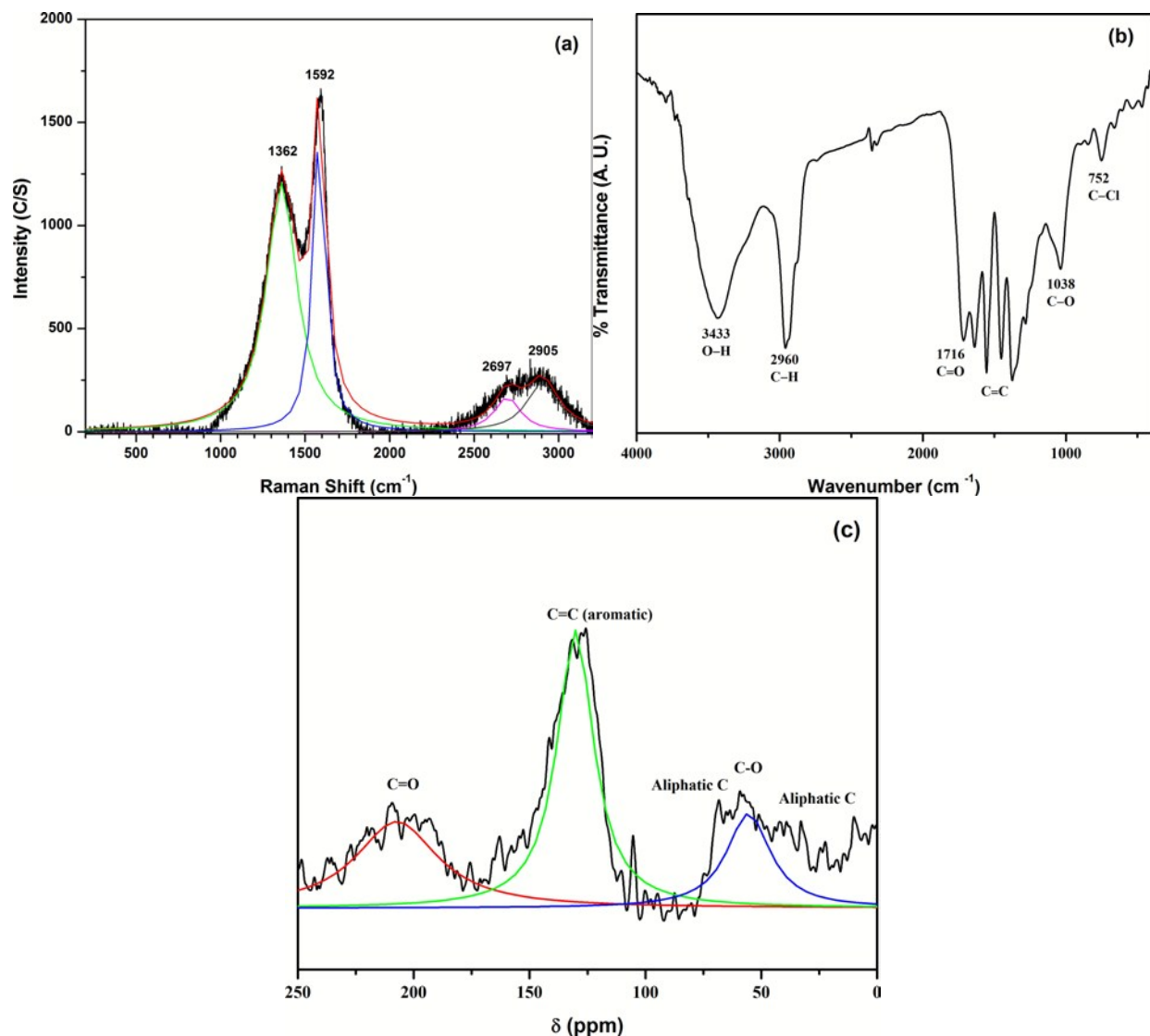


**Fig. 4** Structural and chemical environment illustration of few layered graphene sheets obtained by modified Ullmann reaction using (a) FT-Raman, (b) FT-IR and (c) <sup>13</sup>C solid-state CP-MAS NMR spectroscopy

The obtained product was characterized further by FT-Raman analysis for additional structural exploration. The FT-Raman spectrum of the product (Fig. 4a) revealed four

characteristics peaks in the range, 1000-3000  $\text{cm}^{-1}$ . The peak at 1362  $\text{cm}^{-1}$ , i.e., D-band was attributed to the topological defects or disorder of the obtained graphene sheets mainly due to the introduction of  $sp^3$  character. The G-band observed at 1592  $\text{cm}^{-1}$ , which is the characteristic peak of graphene for its planar configuration of a  $sp^2$  bonded carbon structure, was shifted towards a higher wavelength (compared to a single layer graphene sheet i.e.  $\sim 1582 \text{ cm}^{-1}$ ) due to the increased sheet thickness /number of layers.<sup>35</sup> The broad peak at 2500-3200  $\text{cm}^{-1}$  appeared as a combined peak for 2D (at 2697  $\text{cm}^{-1}$ , second order or overtone of D-band) and D + G (at 2905  $\text{cm}^{-1}$ ) bands mainly due to the irregular layer thickness with a disordered arrangement and *in-situ* functionalization of nanosheets.<sup>22, 36</sup> The effect of the layer thickness and functionalization on the 2D-band was also reported by Hong et al.<sup>37</sup> and Subrahmanyam et al.<sup>16</sup> The in-plane crystalline size calculated using the Ferrari and Robertson formula,  $[(I_D/I_G) = C \cdot L_a^2]$  was 11.9 nm ( $C \approx 0.0055$  for 514 nm).<sup>38</sup>

Generally, the solvothermal synthesis route and acid treatment resulted in a high level of surface functionalization of the carbon products.<sup>39, 40</sup> The observed bands in the FT-IR spectrum of few layered graphene sheets (Fig. 4b) could be assigned to the absorption of different functional groups, including O-H (3433  $\text{cm}^{-1}$ ), C=O (1716–1638  $\text{cm}^{-1}$ ), C=C (1550–1400  $\text{cm}^{-1}$ ), and C-H (2960  $\text{cm}^{-1}$ ).<sup>41</sup> A band in the region, 1038  $\text{cm}^{-1}$ , was associated with the C–O stretching mode. The surface functionalities such as –COOH, –OH, –COOC– and –C–O–C– groups generated during the post-synthesis acid treatment<sup>22</sup>. Nitric acid treatment is also well reported method for the generation of surface oxygen functionalities.<sup>16, 42</sup> The presence of a covalently attached chlorine groups was indicated by the weak adsorption at 752  $\text{cm}^{-1}$ .<sup>43</sup> The covalently bonded chlorine groups mainly resulted from the incomplete reduction of chloroform used as carbon source, and it was also noticed during the synthesis of carbon nanotubes and nano-trees using

dichloromethane and 1, 2-dichlorobenzene as carbon source, respectively.<sup>44, 45</sup> The presence of surface functionality was also evidenced by  $^{13}\text{C}$  MAS-NMR analysis of a few layered graphene sheets. The  $^{13}\text{C}$  MAS-NMR spectrum of few layered graphene sheets (Fig. 4c) showed three major broad peaks, where the peak at  $\sim 56$  ppm was associated mainly with epoxide and hydroxide functionalities.<sup>15</sup> The notable presence of  $sp^2$  hybridized carbon atoms related to the C=C bond in the few layered graphene sheets was illustrated by the strong peak at  $\sim 130$  ppm.<sup>46</sup> The presence of carbonyl groups was also detected by the peak at  $\sim 205$  ppm.<sup>41, 47</sup> The small humps observed in the range, 20-70 ppm, corresponded to the presence of aliphatic carbon. The broadening of the peaks showed the variation in the chemical environment of different carbons atoms.

### 3.5. Textural properties

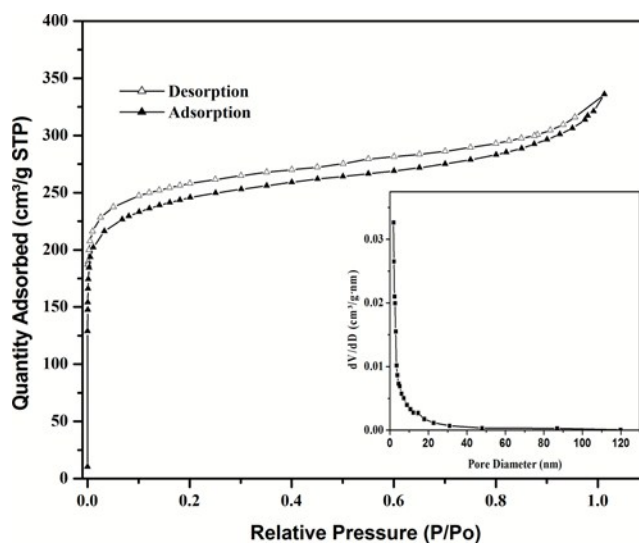


**Fig. 5** N<sub>2</sub> sorption isotherm at 77 K of few layered graphene sheets obtained by modified Ullmann reaction (Inset figure shows the BJH pore size distribution with sharp peak at  $\sim 2$  nm).

The N<sub>2</sub> sorption isotherm at 77 K (Fig. 5) provided information on the specific surface area, porosity and other related properties of the synthesized few layered graphene sheets (Table 1). The measured isotherm exhibited Type IV behavior with a hysteresis loop of Type H4 indicated the adsorption by aggregates of plate-like particles or adsorbents containing slit-shaped pores, mainly due to the capillary condensation between the two layers of graphene.<sup>48, 49</sup> Therefore, the prepared graphene sheets possess a mesoporous nature with a BET surface area of 876 m<sup>2</sup>/g. The surface area of the prepared graphene sheets was not as high as that of the estimated surface area of single layer graphene (2630 m<sup>2</sup> g<sup>-1</sup>), which may be due to the number of layers and aggregated nature of graphene sheets, but almost double than graphene oxide prepared using Hummers method.<sup>15, 50, 51</sup> The three dimensional particle nature of the prepared few layered graphene sheets may be responsible for their high surface area as compared with two dimensional graphene oxide. The inset of Fig. 5 show pore size distribution, which was obtained from the adsorption branch of the nitrogen isotherm, of few layered graphene sheets using the BJH model. The elemental composition (Table 2) of the graphene sheets prepared from chloroform was determined by CHN/O/Cl analysis and confirmed by EDX, which revealed a carbon content of up to 69 % on a weight basis. The graphene sheets also had surface chlorine groups, as indicated by the characteristic adsorption peak of C–Cl at 752 cm<sup>-1</sup> in FT-IR spectrum.

**Table 1** Textural properties of few layered graphene sheets obtained from the modified Ullmann reaction

Specific surface area (m <sup>2</sup> /g)				Pore volume (cm <sup>3</sup> /g)		Average pore diameter (nm)	
S <sub>BET</sub> <sup>a</sup>	S <sub>Langmuir</sub> <sup>b</sup>	S <sub>micro</sub> <sup>c</sup>	S <sub>ext</sub> <sup>d</sup>	V <sub>T</sub> <sup>e</sup>	V <sub>micro</sub> <sup>f</sup>	D <sub>BET</sub> <sup>g</sup>	D <sub>BJH</sub> <sup>h</sup>
876.4	1058.4	565.5	310.9	0.485	0.244	2.21	5.56

<sup>a</sup> Brunauer-Emmer-Teller (BET) surface area.

<sup>b</sup> Langmuir surface area

<sup>c</sup> Micropore surface area, calculated using t -plot method.

<sup>d</sup> External surface area, calculated using t -plot method.

<sup>e</sup> Single point adsorption total pore volume, obtained at P/P<sub>0</sub> = 0.975.

<sup>f</sup> t-Plot micropore volume.

<sup>g</sup> Adsorption average pore diameter, obtained from 4V/A by BET.

<sup>h</sup> Average pore diameter derived from adsorption branch of isotherm and BJH model.

**Table 2** Elemental composition (weight basis) of graphene sheets obtained using chloroform and copper by modified Ullmann reaction determined by CHN/O/Cl and EDX analysis

Elements	CHN/O/Cl analysis	EDX analysis
Carbon	69.40	78.65
Hydrogen	1.90	---
Nitrogen	0.64	---
Oxygen	18.27 (by difference)	17.22
Chlorine	9.79	3.54
Copper	---	0.59



### 3.6. Thermal analysis

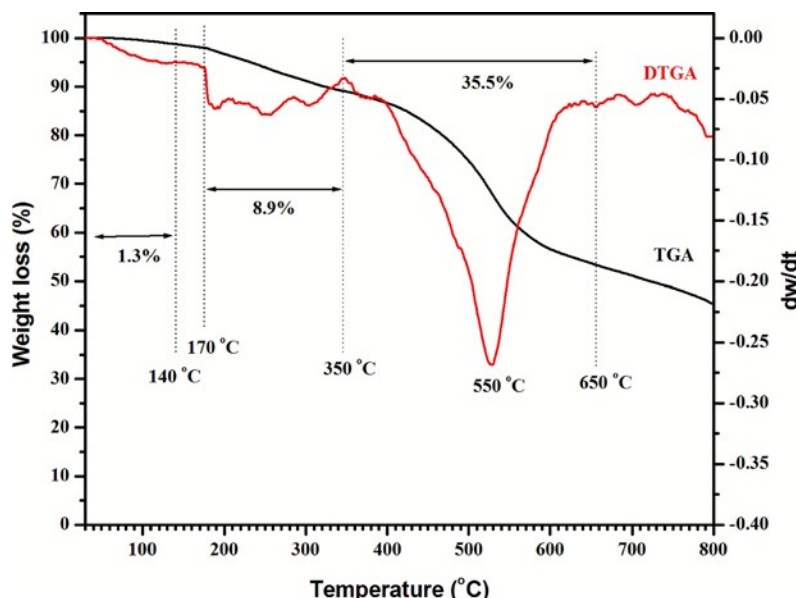


**Fig. 6** TGA and DTGA plots of the few layered graphene sheets obtained using modified Ullmann reaction under  $N_2$  atmosphere.

The thermal stability of prepared graphene sheets was examined by TGA under a nitrogen atmosphere (Fig. 6). Initial minor weight loss of  $\sim 1.3\%$  up to  $140\text{ }^\circ\text{C}$  was due to the evaporation of physisorbed water on few layered graphene sheets. The decomposition of chemisorbed water and surface chloride groups resulted in the second major weight loss ( $\sim 8.9\%$ ) in the range,  $170\text{--}350\text{ }^\circ\text{C}$ . In contrast, the degradation of surface oxygen functionality, including  $-\text{OH}$ ,  $-\text{COOH}$ ,  $\text{C-O-C}$ , and  $\text{C=O}$  etc., of the few layered graphene sheets was observed mainly above  $350\text{ }^\circ\text{C}$ , and resulted in a major weight loss of  $\sim 35.5\%$  centered at  $550\text{ }^\circ\text{C}$ .<sup>52, 53</sup> The decomposition of the surface functionalities of graphene sheets during heat treatment has been well studied by the Choucair et al.<sup>21</sup> using TGA coupled mass spectroscopy. Owing to the high surface functionality, the few layered graphene sheets showed a total weight loss of

~55% at 800 °C under a nitrogen atmosphere. The prepared few layered graphene sheets possess comparative stability as graphene oxide produced from graphite under nitrogen atmosphere.<sup>15, 54</sup>

### 3.7. Growth mechanism

The classical Ullmann reaction involves the copper-catalyzed synthesis of symmetrical biaryls. The mechanism involves the initial formation of active species such as  $\text{Cu}^+$ , which undergoes further oxidative addition with an equivalent of halide, followed by reductive elimination and the formation of a carbon-carbon bond.<sup>23</sup> In the present protocol, the synthesis of graphene sheets was performed under autogenic high pressure conditions. Therefore, it was difficult to analyze the  $\text{Cu}^+$  active compounds formed during the synthesis of few layered graphene sheets. On the other hand, it might be possible to understand the probable growth mechanism of the graphene sheets by knowing the intermediate products.<sup>55</sup> Therefore, the mother liquor recovered after the synthesis of the graphene sheets was analyzed by GC-MS for a qualitative and quantitative determination of the intermediate products. The chemical composition of the recovered solvent determined by GC-MS (Table 3) contained various addition products resulting from C-C bond formation. Shen et al.<sup>56</sup> reported the formation mechanism of carbon nanotubes prepared by the dechlorination pathway. Here, the reductive elimination of chloride from chloroform yielded carbon with metallic copper as the reducing agent. The reaction may involve the formation of organo-copper compounds, which react with the other reactant molecule to form the building block molecules of graphene. The formation of graphene sheets proceeds through the self-assembly of various chloro alkene intermediate compounds (Table 3), which were formed by the breaking of the C-Cl and C-H bonds, and the formation of C-C bonds between two chloroform molecules. GC-MS analysis of the mother

liquor showed that more than 75% of the intermediate product contained 1,3-hexadiene-5-yne (31.74%), tetrachloroethylene (23.99%), hexachlorobutadiene (8.06%), hexachlorobenzene (7.71%) and 1,1,2,2-tetrachloroethane (6.69%), wherein 1,3-hexadiene-5-yne and hexachlorobenzene are the primary building blocks of the graphene structure. The formation of  $sp^2$  hybridized intermediate structures from  $sp^3$  hybridized carbon source during dechlorination reaction have also been reported by Xiong et al.<sup>55</sup> Fig. 7 represents the possible formation mechanism of graphene sheets. The formation of graphene sheets proceeds mainly through two separate processes; one is the formation of building blocks of graphene sheets from chloroform molecules through C–C bond formation, followed by their cyclization or condensation (Fig. 7).<sup>25</sup>

55

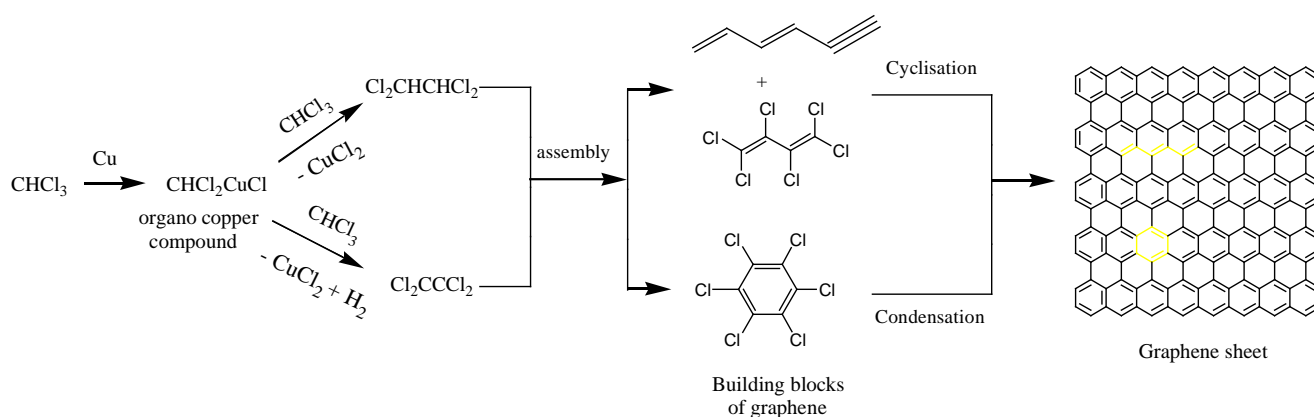


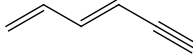
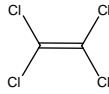
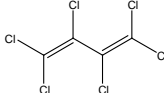
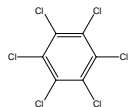
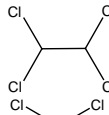
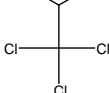
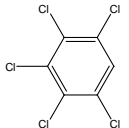
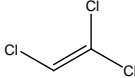
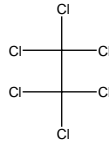
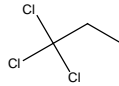
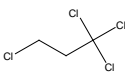
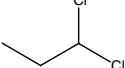
**Fig. 7** Proposed mechanism for the synthesis of graphene sheets, using chloroform as the carbon source and metallic copper as a catalyst based on the modified Ullmann reaction. The colored part in graphene sheet structure shows the building blocks of graphene sheets formation.

No intermediate product with more than six carbon atoms was observed; hence, the addition of chloroform molecules proceeded up to the six carbon atoms only, followed by

interconnection with each other to form graphene sheets.<sup>29</sup> Therefore, under the present reaction conditions, the formation of graphene sheets proceeds by the interconnection of building block molecules and not by the chain polymerization reaction. As indicated by GC-MS, the formation of a carbon product proceeds through the several addition/ condensation reactions. As the molecular size increases, a decrease in the rate of condensation or addition reaction was observed.<sup>57</sup> Therefore, at a particular stage, the rate of reaction of intermediate product formation will be higher than their consumption or conversion to the solid carbon product. Hence, there is a higher likelihood of obtaining the intermediate products, which was confirmed by GC-MS. In a nutshell the accumulation of the carbon product on the copper catalyst limits cyclic C-C bond formation.<sup>22</sup>

The reactions with carbon tetrachloride and dichloromethane as the carbon feedstock were carried out using the same reaction parameters. The product obtained with carbon tetrachloride exhibited horn- and fishbone-like structures with graphene sheets (Fig. S1a and Fig. S2a, ESI<sup>†</sup>). Whereas the foam like structure containing graphene sheets with high agglomeration were obtained using dichloromethane as the carbon source (Fig. S1b and Fig. S2b, ESI<sup>†</sup>). Further characterization, including XRD, FT-IR and elemental composition, of the products obtained using carbon tetrachloride and dichloromethane as carbon sources is provided in the ESI<sup>†</sup>.

**Table 3** Composition of mother liquor obtained after synthesis of the graphene sheets using chloroform and copper by modified Ullmann reaction as determined GC-MS analysis

Sr. No.	Compound name	Composition (wt. %)	Structure
1	1,3-Hexadiene-5-yne	31.74	
2	Tetrachloroethylene	23.99	
3	Hexachlorobutadiene	8.06	
4	Hexachlorobenzene	7.71	
5	1,1,2,2-Tetrachloroethane	6.69	
6	Pentachloroethane	4.39	
7	Pentachlorobenzene	3.84	
8	Trichloroethylene	3.36	
9	Hexachloroethane	3.21	
10	1,1,1-Trichloropropane	3.06	
11	1,1,1,3-Tetrachloropropane	2.51	
12	1,1-Dichloropropane	1.43	

#### 4. Conclusion

A low temperature, single-pot, bottom-up approach for the synthesis of graphene sheets using the modified Ullmann reaction was demonstrated. Aggregated, thin, crumpled graphene sheets with thicknesses of ~2 nm were synthesized successfully from chloroform as the carbon source using solvothermal technique. The formation of graphene sheets proceeded via C-C bond formation with different chlorinated aliphatic and aromatic hydrocarbons as the intermediate products. The formation of graphene sheets proceeds mainly with the addition and cyclization of intermediate alkene compounds instead of the chain polymerization of single carbon atoms. The possible growth mechanism of graphene sheets was also discussed.

#### Acknowledgments

SYS, RSS and HCB are grateful to Council of Scientific and Industrial Research (CSIR), New Delhi, India for the financial support under the Network project CSC-102. SYS and MHC acknowledges to the Ministry of Education, South Korea for financial support by Priority Research Centers Program through the National Research Foundation of Korea (NRF) (2014R1A6A1031189).

† **Electronic supplementary information (ESI) available:** SEM, TEM, XRD, FT-IR, and elemental composition of the products obtained using carbon tetrachloride and dichloromethane as carbon sources.

#### References

1. C.-T. Lin, C.-Y. Lee, H.-T. Chiu and T.-S. Chin, *Langmuir*, 2007, **23**, 12806-12810.
2. M. J. Allen, V. C. Tung and R. B. Kaner, *Chem. Rev.*, 2010, **110**, 132-145.

3. X. Zhuang, Y. Mai, D. Wu, F. Zhang and X. Feng, *Adv. Mater.*, 2015, **27**, 403-427.
4. Z. H. Ni, H. M. Wang, Y. Ma, J. Kasim, Y. H. Wu and Z. X. Shen, *Acs Nano*, 2008, **2**, 1033-1039.
5. K. S. Novoselov, A. K. Geim, S. V. Morozov, D. Jiang, Y. Zhang, S. V. Dubonos, I. V. Grigorieva and A. A. Firsov, *Science*, 2004, **306**, 666-669.
6. K. S. Novoselov, A. K. Geim, S. V. Morozov, D. Jiang, M. I. Katsnelson, I. V. Grigorieva, S. V. Dubonos and A. A. Firsov, *Nature*, 2005, **438**, 197-200.
7. M. I. Katsnelson, K. S. Novoselov and A. K. Geim, *Nat. Phys.*, 2006, **2**, 620-625.
8. A. K. Geim and K. S. Novoselov, *Nat. Mater.*, 2007, **6**, 183-191.
9. Y. Zhang, Y.-W. Tan, H. L. Stormer and P. Kim, *Nature*, 2005, **438**, 201-204.
10. S. Stankovich, D. A. Dikin, G. H. B. Dommett, K. M. Kohlhaas, E. J. Zimney, E. A. Stach, R. D. Piner, S. T. Nguyen and R. S. Ruoff, *Nature*, 2006, **442**, 282-286.
11. H. C. Schniepp, J.-L. Li, M. J. McAllister, H. Sai, M. Herrera-Alonso, D. H. Adamson, R. K. Prud'homme, R. Car, D. A. Saville and I. A. Aksay, *J. Phys. Chem. B*, 2006, **110**, 8535-8539.
12. K. S. Novoselov, D. Jiang, F. Schedin, T. J. Booth, V. V. Khotkevich, S. V. Morozov and A. K. Geim, *P. Natl. Acad. Sci. USA*, 2005, **102**, 10451-10453.
13. C. Berger, Z. Song, X. Li, X. Wu, N. Brown, C. Naud, D. Mayou, T. Li, J. Hass, A. N. Marchenkov, E. H. Conrad, P. N. First and W. A. de Heer, *Science*, 2006, **312**, 1191-1196.
14. T. Ohta, A. Bostwick, T. Seyller, K. Horn and E. Rotenberg, *Science*, 2006, **313**, 951-954.

15. S. Stankovich, D. A. Dikin, R. D. Piner, K. A. Kohlhaas, A. Kleinhammes, Y. Jia, Y. Wu, S. T. Nguyen and R. S. Ruoff, *Carbon*, 2007, **45**, 1558-1565.
16. K. S. Subrahmanyam, S. R. C. Vivekchand, A. Govindaraj and C. N. R. Rao, *J. Mater. Chem.*, 2008, **18**, 1517-1523.
17. J. Wang, M. Zhu, R. A. Outlaw, X. Zhao, D. M. Manos and B. C. Holloway, *Carbon*, 2004, **42**, 2867-2872.
18. P. Song, X. Y. Zhang, M. X. Sun, X. L. Cui and Y. H. Lin, *Rsc Adv*, 2012, **2**, 1168-1173.
19. S. Y. Sawant, R. S. Somani and H. C. Bajaj, *Carbon*, 2010, **48**, 668-672.
20. S. Y. Sawant, R. S. Somani, B. L. Newalkar, N. V. Choudary and H. C. Bajaj, *Mater. Lett.*, 2009, **63**, 2339-2342.
21. M. Choucair, P. Thordarson and J. A. Stride, *Nat. Nanotechnol.*, 2009, **4**, 30-33.
22. S. Y. Sawant, R. S. Somani, S. S. Sharma and H. C. Bajaj, *Carbon*, 2014, **68**, 210-220.
23. F. Ullmann, *Berichte der deutschen chemischen Gesellschaft*, 1903, **36**, 2382-2384.
24. Y. Xie, Q. Huang and B. Huang, *Carbon*, 2010, **48**, 2023-2029.
25. G. Hu, D. Ma, M. Cheng, L. Liu and X. Bao, *Chem. Commun.*, 2002, 1948-1949.
26. Y. Ni, M. Shao, Y. Tong, G. Qian and X. Wei, *J. Solid State Chem.*, 2005, **178**, 908-911.
27. Z. Ju, T. Wang, L. Wang, Z. Xing, L. Xu and Y. Qian, *Carbon*, 2010, **48**, 3420-3426.
28. G. Xi, M. Zhang, D. Ma, Y. Zhu, H. Zhang and Y. Qian, *Carbon*, 2006, **44**, 734-741.
29. Q. Kuang, S.-Y. Xie, Z.-Y. Jiang, X.-H. Zhang, Z.-X. Xie, R.-B. Huang and L.-S. Zheng, *Carbon*, 2004, **42**, 1737-1741.
30. X. Lu, J. Wu, T. Lin, D. Wan, F. Huang, X. Xie and M. Jiang, *J. Mater. Chem.*, 2011, **21**, 10685-10689.



31. D. Banerjee, S. Mukherjee and K. K. Chattopadhyay, *Appl. Surf. Sci.*, 2011, **257**, 3717-3722.
32. T. Itoh, *Thin Solid Films*, 2011, **519**, 4589-4593.
33. Y. Wu, P. Qiao, T. Chong and Z. Shen, *Adv. Mater.*, 2002, **14**, 64-67.
34. M. J. McAllister, J.-L. Li, D. H. Adamson, H. C. Schniepp, A. A. Abdala, J. Liu, M. Herrera-Alonso, D. L. Milius, R. Car, R. K. Prud'homme and I. A. Aksay, *Chem. Mater.*, 2007, **19**, 4396-4404.
35. G. Srinivas, Y. Zhu, R. Piner, N. Skipper, M. Ellerby and R. Ruoff, *Carbon*, 2010, **48**, 630-635.
36. T. Peng, H. Lv, D. He, M. Pan and S. Mu, *Sci. Rep.*, 2013, **3**.
37. N. Hong, B. Wang, L. Song, S. Hu, G. Tang, Y. Wu and Y. Hu, *Mater. Lett.*, 2012, **66**, 60-63.
38. A. C. Ferrari and J. Robertson, *Phys. Rev. B*, 2000, **61**, 14095-14107.
39. Y. Z. Jin, C. Gao, W. K. Hsu, Y. Zhu, A. Huczko, M. Bystrzejewski, M. Roe, C. Y. Lee, S. Acquah, H. Kroto and D. R. M. Walton, *Carbon*, 2005, **43**, 1944-1953.
40. S. Y. Sawant, R. S. Somani, H. C. Bajaj and S. S. Sharma, *J. Hazard. Mater.*, 2012, **227-228**, 317-326.
41. Y. Si and E. T. Samulski, *Nano Lett.*, 2008, **8**, 1679-1682.
42. C. Moreno-Castilla, M. A. Ferro-Garcia, J. P. Joly, I. Bautista-Toledo, F. Carrasco-Marin and J. Rivera-Utrilla, *Langmuir*, 1995, **11**, 4386-4392.
43. H. Hu, B. Zhao, M. A. Hamon, K. Kamaras, M. E. Itkis and R. C. Haddon, *J. Am. Chem. Soc.*, 2003, **125**, 14893-14900.

44. S. Y. Brichka, G. P. Prikhod'ko, Y. I. Sementsov, A. V. Brichka, G. I. Dovbeshko and O. P. Paschuk, *Carbon*, 2004, **42**, 2581-2587.
45. Z. Yao, X. Zhu, X. Li and Y. Xie, *Carbon*, 2007, **45**, 1566-1570.
46. H. He, T. Riedl, A. Lerf and J. Klinowski, *J. Phys. Chem.*, 1996, **100**, 19954-19958.
47. M.-M. Titirici, M. Antonietti and N. Baccile, *Green Chem.*, 2008, **10**, 1204-1212.
48. F. Rouquerol, J. Rouquerol and K. Sing, in *Adsorption by Powders and Porous Solids*, eds. F. Rouquerol, J. Rouquerol and K. Sing, Academic Press, London, 1999, DOI: <http://dx.doi.org/10.1016/B978-012598920-6/50002-6>, pp. 1-26.
49. F. Rouquerol, J. Rouquerol and K. Sing, in *Adsorption by Powders and Porous Solids*, eds. F. Rouquerol, J. Rouquerol and K. Sing, Academic Press, London, 1999, DOI: <http://dx.doi.org/10.1016/B978-012598920-6/50008-7>, pp. 191-217.
50. Y. Zhu, S. Murali, W. Cai, X. Li, J. W. Suk, J. R. Potts and R. S. Ruoff, *Adv. Mater.*, 2010, **22**, 3906-3924.
51. Z. Pei, L. Li, L. Sun, S. Zhang, X.-q. Shan, S. Yang and B. Wen, *Carbon*, 2013, **51**, 156-163.
52. T. Yang, L.-h. Liu, J.-w. Liu, M.-L. Chen and J.-H. Wang, *J. Mater. Chem.*, 2012, **22**, 21909-21916.
53. N. Wu, X. She, D. Yang, X. Wu, F. Su and Y. Chen, *J. Mater. Chem.*, 2012, **22**, 17254-17261.
54. C. Yuan, W. Chen and L. Yan, *J. Mater. Chem.*, 2012, **22**, 7456-7460.
55. Y. Xiong, Y. Xie, Z. Li, C. Wu and R. Zhang, *Chem. Commun.*, 2003, 904-905.
56. J. Shen, Z. Huang, J. Li, L. Gao, H. Zhou and Y. Qian, *Carbon*, 2005, **43**, 2823-2826.

57. X. Yang, X. Dou, A. Rouhanipour, L. Zhi, H. J. Räder and K. Müllen, *J. Am. Chem. Soc.*, 2008, **130**, 4216-4217.